Removal of Polycyclic Aromatic Hydrocarbons from Water Using Mn(III)-Based Advanced Oxidation Process

Jian Fang[1]; Renzun Zhao, Ph.D., M.ASCE[2]; Balaji Rao, Ph.D.[3]; Magdalena Rakowska, Ph.D.[4]; Dimitrios Athanasiou[5]; Kayleigh Millerick, Ph.D.[6]; Suying Wei, Ph.D.[7]; Xiangyang Lei, Ph.D.[8]; Helen H. Lou, Ph.D.[9]; and Danny D. Reible, Ph.D., M.ASCE[10]

Abstract: Floods have the potential to resuspend polycyclic aromatic hydrocarbons (PAHs) laden sediments and potentially impact drinking water intakes. This work identifies optimal operating conditions for the PAH removal from water using a combined permanganate (Mn(VII))/bisulfite advanced oxidation process (AOP). PAHs in aqueous solutions containing humic acid (HA) were treated using a combination of permanganate and bisulfite at different molar ratios. Results showed that the Mn(VII)/bisulfite AOP was an effective method to remove priority PAHs, but the dosage needs to be carefully controlled to avoid excessive by-products and reduce treatment costs. The optimal reaction conditions [$C_{[16PAHs]}$:$C_{[KMnO_4]}$:$C_{[NaHSO_3]}$ = 1:30:60 ($m_{[16PAHs]}$:$m_{[KMnO_4]}$:$m_{[NaHSO_3]}$ = 1:22:29) and 10 min <= reaction time < 30 min] were identified within a wide pH range (5.0–8.0). High removal efficiencies (85%–100%) were achieved for typically refractory high molecular weight PAHs, including pyrene (PYR), chrysene (CHRY), benzo[a]anthracene (B[a]A), benzo[b]fluoranthene (B[b]F), benzo[k]fluoranthene (B[k]F), benzo[a]pyrene (B[a]P), and dibenzo[a,h]anthracene (D[ah]A). The concentration of B[a]P was reduced to below 0.2 μg/L from an initial concentration of 0.8 μg/L in less than 30 min, and a 2 mg-OC/L concentration of HA had minimal effect on the effectiveness of AOP. The maximum concentration level of B[a]P is specified as 0.2 μg/L, according to National Primary Drinking Water Regulations issued by the EPA. Overall, the Mn(VII)/bisulfite AOP represents a promising technology for PAH removal to below minimum EPA drinking water standards in emergency scenarios, although the control of the dosages of permanganate and bisulfite is required. **DOI: 10.1061/(ASCE)EE.1943-7870.0001845.**

Author keywords: Polycyclic aromatic hydrocarbons; Advanced oxidation process; Potassium permanganate; Sodium bisulfite; Humic acid; Drinking water.

Introduction

Polycyclic aromatic hydrocarbons (PAHs) are well-known persistent organic pollutants that resist degradation and exert toxic effects on the environment (Qu et al. 2019). The United States EPA has categorized 16 PAHs as priority contaminants based on their potential risks for human exposure, toxicity, and frequency of occurrence at hazardous waste sites (Mojiri et al. 2019). Table 1 showed that the toxicity equivalency factors of LMW PAHs (FLU, ACE, ACY, and PHEN) are 0.001, indicating that the toxicities of LMW PAHs are three orders of magnitudes lower than that of B[a]P. Soil is one of the most important reservoirs of PAHs, whose half-lives in soils range from years to decades (Yurdakul et al. 2019). PAHs are highly hydrophobic and, when dissolved, tend to be adsorbed rapidly by suspended particulate matter in water (Sun et al. 2009). Once PAHs are adsorbed, suspended particulate matter serves as a transportation medium for PAHs, distributing the pollutants over large areas via rivers and subsequently depositing on sediments, which can be generally regarded as a sink for PAHs (Li et al. 2019).

[1]Dan F. Smith Dept. of Chemical and Biomolecular Engineering, Lamar Univ., 4400 MLK Blvd., P.O. Box 10053, Beaumont, TX 77710. Email: jfang@lamar.edu

[2]Assistant Professor, Dept. of Civil, Architectural, and Environmental Engineering, North Carolina A&T State Univ., 1601 E. Market St., Greensboro, NC 27411. Email: rzhao@ncat.edu

[3]Dept. of Civil, Environmental, and Construction Engineering, Texas Tech Univ., 1010 Boston Ave., Lubbock, TX 79409. ORCID: https://orcid.org/0000-0003-2388-3670. Email: balaji.rao@ttu.edu

[4]Dept. of Civil, Environmental, and Construction Engineering, Texas Tech Univ., 1010 Boston Ave., Lubbock, TX 79409. Email: magdalena.rakowska@ttu.edu

[5]Dept. of Civil, Environmental, and Construction Engineering, Texas Tech Univ., 1010 Boston Ave., Lubbock, TX 79409. Email: Dimitrios.Athanasiou@ttu.edu

Note. This manuscript was submitted on May 5, 2020; approved on September 25, 2020; published online on January 7, 2021. Discussion period open until June 7, 2021; separate discussions must be submitted for individual papers. This paper is part of the ***Journal of Environmental Engineering***, © ASCE, ISSN 0733-9372.

[6]Assistant Professor, Dept. of Civil, Environmental, and Construction Engineering, Texas Tech Univ., P.O. Box 41023, Lubbock, TX 79409–1023. Email: kayleigh.millerick@ttu.edu

[7]Associate Professor, Dept. of Chemistry and Biochemistry, Lamar Univ., 4400 MLK Blvd., P.O. Box 10009, Beaumont, TX 77710. Email: suying.wei@lamar.edu

[8]Associate Professor and Department Chair, Dept. of Chemistry and Biochemistry, Lamar Univ., 4400 MLK Blvd., P.O. Box 10009, Beaumont, TX 77710. Email: xiangyang.lei@lamar.edu

[9]Professor, Dan F. Smith Dept. of Chemical and Biomolecular Engineering, Lamar Univ., 4400 MLK Blvd., P.O. Box 10053, Beaumont, TX 77710 (corresponding author). Email: hhlou@lamar.edu; Helen.lou@lamar.edu

[10]Professor and Donovan Maddox Distinguished Engineering Chair, Dept. of Civil, Environmental, and Construction Engineering, Texas Tech Univ., P.O. Box 41023, Lubbock, TX 79409−1023. Email: danny.reible@ttu.edu

Table 1. Properties and toxicity equivalency factors of 16 PAHs included in the USEPA priority pollutant list

PAHs	Abbreviation[a]	Molecular weight (MW)[a] (g/mol)	Molecular formula (MF)[a]	Solubility in H_2O (25°C)[a] (μg/L)	Vapor pressure (VP)[a] (mm Hg 25°C)	Log K_{ow}[a]	Toxicity equivalency factors (TEF)[b,c]
Naphthalene	NAP	128.17	$C_{10}H_8$	31,000	8.70×10^{-02}	3.30	—
Acenaphthylene[d]	ACY	152.20	$C_{12}H_8$	3,930	2.10×10^{-04}	4.07	0.001
Acenaphthene	ACE	154.21	$C_{12}H_{10}$	3,900	1.50×10^{-04}	3.98	0.001
Fluorene	FLU	166.22	$C_{13}H_{10}$	1,690	3.20×10^{-04}	4.18	0.001
Phenanthrene	PHEN	178.23	$C_{14}H_{10}$	1,100	6.80×10^{-04}	4.45	0.001
Anthracene	ANTH	178.23	$C_{14}H_{10}$	43.4	1.50×10^{-06}	4.45	0.01
Fluoranthene	FLTH	202.26	$C_{16}H_{10}$	200	2.60×10^{-06}	4.90	0.001
Pyrene	PYR	202.26	$C_{16}H_{10}$	135	2.50×10^{-06}	4.88	0.001
Benzo[a]anthracene	B[a]A	228.29	$C_{18}H_{12}$	9.4	1.30×10^{-09}	5.61	0.1
Chrysene	CHRY	228.29	$C_{18}H_{12}$	2	1.30×10^{-09}	5.16	0.01
Benzo[b]fluoranthene	B[b]F	252.32	$C_{20}H_{12}$	1.5	2.80×10^{-12}	6.04	0.1
Benzo[k]fluoranthene	B[k]F	252.32	$C_{20}H_{12}$	0.8	7.00×10^{-11}	6.06	0.1
Benzo[a]pyrene	B[a]P	252.32	$C_{20}H_{12}$	1.62	2.80×10^{-12}	6.06	1
Dibenzo[a,h]anthracene	D[ah]A	278.35	$C_{22}H_{14}$	2.49	1.80×10^{-13}	6.84	5
Benzo[g,h,i]perylene[d]	B[ghi]P	276.34	$C_{22}H_{12}$	0.26	1.60×10^{-12}	6.50	0.01
Indeno[1,2,3-c,d]pyrene[d]	IND	276.34	$C_{22}H_{12}$	0.19	6.30×10^{-14}	6.58	0.1

[a]Data from the US National Center for Biotechnology Information (2019).
[b]Data from Department of Health & Human Services, Public Health Service (DHHS 1999).
[c]The cancer potency of Benzo[a]pyrene is 7.3 mg/kg/day. USEPA has developed TEF, and the cancer potency of the other carcinogenic PAHs can be estimated (divide by TEF) based on it.
[d]ACY, B[ghi]P, and IND cannot be individually evaluated in this study due to low detection and coelution in the analytical method.

Climate change is leading to an increased frequency of natural disasters (Zoppini et al. 2019), including hurricanes. Temporary hurricane flooding may drastically increase water column heights and surface water migration, which may release and transport hazardous materials present in sediments. One such example occurred during Hurricane Harvey, which led to record rainfall in Beaumont, Texas, from August 29 to 31, 2017. Because of the unprecedented flooding, the primary pump station of Beaumont's water treatment plant (WTP) was taken offline on August 30th and resumed on September 7th. During this 7-day window, a temporary pump station upstream of the Brakes Bayou provided water to the WTP (Amadeo 2019). Downstream about 800 m from the temporary water intake, the lower reaches of the Brakes Bayou are bound to the west by a superfund site containing substantial PAH contamination and an island (CB&I) to the east with significant industrial activity, posting the potential for PAHs' mobilization into a surface water body serving as a temporary water source. However, very few technologies to date have been identified or evaluated to mitigate the negative water quality events caused by natural disasters. Developing such techniques are necessary to provide safe water for residents in emergencies.

To remove organic compounds from water, the effectiveness of conventional oxidants, including chlorine (Deborde and von Gunten 2008; Wang et al. 2011), chlorine dioxide (Hoigné and Bader 1994; Huber et al. 2005), hydrogen peroxide (Liao et al. 2019), permanganate (Brown et al. 2003; Hu et al. 2010; Jiang et al. 2012; Kao et al. 2008; Sun et al. 2013; Zhang et al. 2013), and ozone (Ates and Argun 2018; Von Gunten 2003; Zimmermann et al. 2011) were reviewed. Potassium permanganate ($KMnO_4$) has the advantages of easy handling, effectiveness, relatively low cost, and comparative stability over a wide pH range, and it is a promising technology for the oxidative removal of various phenolic compounds [bisphenol A, triclosan, estrone, 17β-estradiol, estriol, chlorophenols, and bromophenols (Anipsitakis et al. 2006; Kochany and Lipczynska-Kochany 1992; Perez-Benito et al. 1996; Sun et al. 2016c)] and trace organics that contain electron-rich moieties [amino groups, thiols, and ethers (Zazo et al. 2005)].

The mechanisms of organics contaminant oxidation by $KMnO_4$ varies with the pH. Acid-catalyzed reactions occur below a pH of 5.0, uncatalyzed reactions are dominant when the pH is between 6.0 and 9.0, and base-catalyzed reactions occur at pH higher than 10.0. These pH ranges correspond with the dominant species of manganese present; species include permanganate (Hu et al. 2010; Thabaj et al. 2007), manganese dioxide (MnO_2) (Perez-Benito 2011), cryptomelane-type manganese(III/IV) (Xiao et al. 2013), and Mn_3O_4 (Chowdhury et al. 2009). Permanganate oxidation is highly reactive under acidic conditions as acid-catalysis generates electrophilic intermediate products, which are strongly attracted to the electrons of organic compounds and promote hydroxylation, hydrolysis, or ring cleavage reactions (Abdullah et al. 2014).

Permanganate alone is an ineffective PAH oxidant because of its inability to oxidize benzene rings (Waldemer and Tratnyek 2006), the basic building block of all PAHs. However, Sun et al. (2015, 2016a, b, c, 2018) reported that a large amount of soluble aquo and/or hydroxo Mn(III) (i.e., noncomplexed with ligands other than H_2O and ·OH) could be generated when permanganate is combined with bisulfite ($NaHSO_3$), a commonly used reductant. This Mn(VII)/bisulfite system, a relatively new advanced oxidation process (AOP), has been shown to oxidize phenol when $C_{[contaminants]}$:$C_{[KMnO_4]}$:$C_{[NaHSO_3]}$ (μmol/L) = 1:50:250. At these concentrations, phenol was rapidly (<20 s) degraded by the produced hydroxo Mn(III) over a wide pH range.

This paper explores the potential of using an Mn(VII)/bisulfite AOP for PAH removal under conditions pertinent to emergency surface water treatment, specifically investigating the influence of solution chemistry on the degradation of 13 PAHs. Parameters investigated include humic acid (ubiquitous in natural water), solution pH, the molar concentration ratio of reactants, and reaction time (RT). Finally, this study identifies optimal operating conditions to maximize PAH removal while minimizing the generation of by-products and treatment costs.

Materials and Methods

Materials

Humic acid sodium salt powder (HA) was obtained from Alfa Aesar (Haverhill, Massachusetts). Aluminum oxide (basic, Brockmann I, for chromatography, 50–200 μm, 60 Å, ACROS Organics, Fair Lawn, New Jersey) was activated by heating (130°C for 16 h) and deactivated with 10%–12% (w/w) water. Sodium sulfate anhydrous (Granular/Certified ACS, Fisher Chemical, Waltham, Massachusetts) was dried for 4 h at 400°C in a shallow tray and stored in a sealed desiccator. Granular sodium bisulfite was obtained from Macron Fine Chemicals (Italy). Potassium permanganate was obtained from Fisher Chemical (Waltham, Massachusetts). A PAH standard solution mix containing the 16 PAHs designated EPA priority pollutants was obtained from Accustandard (New Haven, Connecticut). This mix contained 0.2 mg/mL of each PAH compound in dichloromethane:methanol (CH_2Cl_2:MeOH, 50:50, v/v). All other reagents used in these experiments were reagent grade and were used without further treatment.

Dichloromethane (DCM) ≥ 99.8% stabilized, HiPerSolv CHROMANORM for HPLC, acetonitrile (ACN) anhydrous (max. 0.003% H_2O) ≥ 99.9%, HiPerSolv CHROMANORM, super gradient grade for HPLC, VWR Chemicals BDH (Denver, Colorado), and acetone, Optima, for HPLC and GC, were obtained from Fisher Scientific (Fair Lawn, New Jersey). Deionized (D.I.) water was used in all the experiments (pH 6.5).

Glassware was purchased from VWR (Radnor, Pennsylvania). The glassware was washed with detergent and D.I. water and then rinsed three times with acetone and DCM, respectively. The glassware was dried at 120°C for 4 h.

Preparation of Humic Acid Solution

A total of 2 g of dry HA powder was weighed and transferred into a 500 mL beaker containing D.I. water. The solution was stirred on a magnetic plate overnight and then filtered through a PTFE syringe filter (Waters Acrodisc, Milford, Massachusetts, 13 mm, 0.45 μm). The pH of the HA solution was adjusted to 7.0 (the average pH value of the Neches River over the last five years) (TCEQ 2017) using 1 M solutions of HCl and NaOH. The resulting solution was stored in the dark at 4°C and used for PAH experiments and measurements of dissolved organic carbon (DOC) and total organic carbon (TOC). Humic acid concentrations were reported as milligrams of organic carbon per liter (mg-OC/L).

PAH Extraction Using Liquid-Liquid Extraction and PAH Recovery

A total of 40 mL of an aqueous solution containing PAHs were added into a 125 mL separatory funnel. The funnel was capped, and the sample was shaken vigorously by hand for 1 min after 5 mL DCM was added and then left to stand for 15 min, and the organic phase was collected. This process was repeated three times, and sequential extracts were combined and evaporated via Rocket evaporator (The Genevac Rocket Evaporation System, Ipswich, England) at 30°C and a 190 mbar vacuum until only 1–2 mL DCM remained. Interfering compounds were removed by the liquid-solid chromatography method using a 1:3 (v/v) sodium sulfate anhydrous-aluminum oxide column before Rocket evaporation. Evaporated extracts were transferred to 15 mL ACN and concentrated to 1 mL in the Rocket evaporator (0°C and 32 mbar vacuum). Finally, sample volumes were further reduced to 0.1–0.2 mL under a gentle stream of nitrogen.

To validate the recovery of PAHs by the LLE method, two identical concentrated solutions of 16 PAHs were prepared. One was analyzed directly by HPLC. The second was added to 40 mL water, shaken for 24 h at 20°C, extracted by LLE, and analyzed by HPLC. All the experiments were conducted in triplicate.

AOP Batch Experiments

The PAH standard solution was diluted in ACN to a working stock concentration of 40 μg/L and stored at −20°C in the dark. To ensure all except for two PAHs (B[ghi]P and IND) would dissolve in water, most experiments were conducted using a 0.8 μg/L PAH solution unless stated otherwise. The physicochemical properties of 16 PAHs were shown in Table 1.

To perform an initial screening experiment, 40 μg/L PAH solution and HA solution were diluted by D.I.water to 0.8 μg/L PAH solutions containing 0 and 2 mg-OC/L HA. The pH value of the solution was gradually adjusted using 1 M HCl and NaOH. Potassium permanganate and sodium bisulfite were added to the solutions (molar concentration ratios of $C_{[16PAHs]}$:$C_{[KMnO_4]}$:$C_{[NaHSO_3]}$ fixed at 1:50:250) gradually and stirred by the magnetic stirrer for 5 min. Then, the mixture was filtered using glass fiber syringe filters (Waters Acrodisc, Milford, Massachusetts, 25 mm, 1 μm) and extracted by LLE. The top aqueous phase containing Mn(II) and sulfate were analyzed, and the bottom extracted phase containing 16 PAHs was analyzed. The solution, containing 0.8 μg/L PAH solutions and 2 mg-OC/L HA at pH = 7.0 but no $KMnO_4$ nor $NaHSO_3$, was referred to as no oxidant. The solutions with oxidants and the solutions of no oxidants were treated identically to experimental systems. All the experiments were conducted in triplicate.

The effects of pH, molar concentration ratios of PAHs and $KMnO_4$ ($C_{[16PAHs]}$:$C_{[KMnO_4]}$), molar concentration ratios of $KMnO_4$ and $NaHSO_3$ ($C_{[KMnO_4]}$:$C_{[NaHSO_3]}$), and reaction time (RT) on PAH oxidation were sequentially investigated in this study. Firstly, pH values of 5.0, 6.0, 7.0, and 8.0 (target values) were investigated when $C_{[16PAHs]}$:$C_{[KMnO_4]}$:$C_{[NaHSO_3]}$ = 1:50:250 and RT = 5 min. Secondly, molar concentration ratios of 1:40, 1:30, 1:20, and 1:10 ($C_{[16PAHs]}$:$C_{[KMnO_4]}$) were investigated at optimum pH, $C_{[KMnO_4]}$:$C_{[NaHSO_3]}$ = 1:5, and RT = 5 min. Thirdly, molar concentration ratios of 1:4, 1:3, 1:2, and 1:1 ($C_{[KMnO_4]}$:$C_{[NaHSO_3]}$) were investigated at an optimum pH and $C_{[16PAHs]}$:$C_{[KMnO_4]}$ ratio, and RT = 5 min. Finally, the reaction time = 0.5, 1.0, 2.0, 5.0, 15.0, and 30.0 min were investigated at the optimum and $C_{[16PAHs]}$:$C_{[KMnO_4]}$:$C_{[NaHSO_3]}$ ratio. All the experiments were conducted in triplicate.

PAH Quantification

PAH concentrations were measured by HPLC with fluorescence detection (EPA 1986). Analyses were performed with an Agilent Technologies 1260 Infinity (Santa Clara, California) high-performance liquid chromatography (HPLC) equipped with a fluorescence detector (1260 FLD spectra). Eight different calibration standards (1.0, 2.0, 5.0, 10.0, 20.0, 50.0, 100.0, and 200.0 ng/mL in ACN) were used for quantification. Analytes were separated using a Phenomenex (Torrance, California) Luna 5 μm C18 column (250 × 4.6 mm) maintained at 40°C and a flow rate of 1 mL/min. The isocratic mobile phase consisted of ACN and Milli-Q high purity water (70:30, v/v). The injection volume was 10 μL, and sample runs were 42 min. This method can quantify only 13 of the 16 PAHs because ACY does not fluoresce and cannot be detected, and the peaks of B[ghi]P and IND overlap. The FLD periods and the excitation/emission wavelength pairs (nm/nm) for each PAH compound were shown in Table 2.

Table 2. Fluorescence detector periods and detection wavelength program for HPLC measurement of PAHs

Time (min)	Excitation wavelength (nm)	Emission wavelength (nm)	Detected compounds
0.00–8.90	280	340	NAP
8.90–12.12	260	352	FLU, ACE, and PHEN
12.12–13.25	260	420	ANTH
13.25–15.10	260	440	FLTH
15.10–30.00	260	420	PYR, CHRY, B[a]A, B[b]F, B[k]F, and B[a]P
30.00–42.00	305	430	D[ah]A and B[ghi]P+IND

ICP-MS and IC Procedures

The oxidation reaction of Mn(VII)/bisulfite generated some by-products, and the main by-products were Mn(II) and sulfate.

After the oxidation reaction, MnO_2 was filtered out, and the filtered solution was divided into two parts for Mn(II) and SO_4^{2-} analyses. Mn(II) was analyzed using an ELAN 9000 ICP-MS (PerkinElmer, Shelton, Connecticut) following EPA Method 220.8 (EPA 1994). SO_4^{2-} was analyzed by ion chromatography (Thermo ion chromatography, Thermo Fisher Scientific, Waltham, Massachusetts) using a CD25 conductivity detector equipped with a Dionex Ionpac AS14A column, following EPA Method 300.0 (Pfaff 1993).

Data Analysis

The removal efficiency of each PAH compound via Mn(VII)/bisulfite AOP was calculated

$$RE = \left(\frac{C_{\text{no oxidant}} - C_e}{C_{\text{no oxidant}}}\right) \tag{1}$$

where $C_{\text{no oxidant}}$ (μg/L) = concentration of each PAH compound without oxidant; and C_e (μg/L) = residual concentration of each PAH compound. The $C_{\text{no oxidant}}$ (μg/L) was calculated using the following equation:

$$C_{\text{no oxidant}} = C_0 \times CF_{2\,mg-OC/L} \tag{2}$$

where C_0 (μg/L) = initial concentration of each PAH compound (0.8 μg/L in this study); and $CF_{2\,mg-OC/L}$ = LLE extraction efficiency of each PAH compound from solutions containing 2 mg-OC/L HA. The values of $CF_{2\,mg-OC/L}$ for each PAH compound were listed in Table 3.

The residual concentration of each PAH compound (μg/L) was calculated using the following equation:

$$C_e = \frac{\left(\frac{\text{Mass}_{\text{Residual PAH}}}{V}\right)}{CF_{0\,mg-OC/L}} \tag{3}$$

where $\text{Mass}_{\text{residual PAH}}$ (μg) was calculated for each PAH compound from the HPLC calibration curve; V (L) = solution volume; and $CF_{0\,mg-OC/L}$ = LLE extraction efficiency of each PAH compound from solutions without HA. The values of $CF_{0\,mg-OC/L}$ for each PAH compound are listed in Table 3.

The Mn(II) concentration (mg/L) generated in theory was calculated

Table 3. LLE extraction efficiencies of each PAH compound from aqueous solutions with different concentrations of HA

PAHs	0 mg-OC/L HA solution (%)	2 mg-OC/L HA solution (%)
Naphthalene	69	62
Acenaphthene	73	66
Fluorene	73	68
Phenanthrene	72	67
Anthracene	71	63
Fluoranthene	77	68
Pyrene	79	68
Benzo[a]anthracene	88	72
Chrysene	89	74
Benzo[b]fluoranthene	91	72
Benzo[k]fluoranthene	92	71
Benzo[a]pyrene	83	71
Dibenzo[a,h]anthracene	97	60

Note: PAHs containing 0 and 2 mg-OC/L HA solutions were shaken for continuously 24 h and extracted by the LLE method.

$$C_{T\,Mn(II)} = C_{\text{total PAHs}} \times R \times MW_{Mn} \tag{4}$$

where $C_{\text{total PAHs}}$ (mmol/L) = total molar concentration of the 16 PAH compounds; R = molar concentration ratio of $KMnO_4$ and total PAHs ($C_{[KMnO_4]}$:$C_{[PAHs]}$); and MW_{Mn} = molecular weight of Mn (mg/mmol). The total concentration of PAHs (mmol/L) can be calculated using the following equation:

$$C_{\text{total PAHs}} = \sum \frac{C_{0\,\text{PAHs}}}{MW_{i=16}} \tag{5}$$

where $MW_{i=16}$ = molecular weight of the 16 PAH compounds (mg/mmol).

The sulfate concentration (mg/L) generated in theory was calculated

$$C_{T\,SO_4^{2-}} = C_{T\,Mn(II)} \times R \times MW_{\text{sulfate}} \tag{6}$$

where R = molar concentration ratio of $NaHSO_3$ and $KMnO_4$ ($C_{[NaHSO_3]}$:$C_{[KMnO_4]}$); and MW_{sulfate} = molecular weight of sulfate (mg/mmol).

Results and Discussion

Low molecular weight (LMW) PAHs (two or three aromatic rings) and high molecular weight (HMW) PAHs (more than three aromatic rings) showed different behavior in oxidation experiments. Anthracene (ANTH) also behaved differently than other small PAHs. The National Primary Drinking Water Regulations (NPDWRs) 40 CFR § 141.61 (EPA 2012) specifies the federal regulation for the maximum contaminant levels (MCL) of organic contaminants in community water systems and nontransient, noncommunity water systems. Among the PAHs investigated, only MCL of B[a]P is specified as 0.2 μg/L; therefore, the C_e of B[a]P is legally enforceable as a primary standard and can serve as a benchmark for the effectiveness of the Mn(VII)/bisulfite AOP in the experiments. Besides, the National Secondary Drinking Water Regulations (NPSWRs) also specifies that Mn(II) secondary maximum contaminant level (SMCL) is 0.050 mg/L, and the sulfate SMLC is 250.0 mg/L for drinking water (USEPA 2009). Note that the SMCL recommended in the NPSWRs are set for esthetic reasons and are not enforceable by EPA (Abernathy et al. 2003) but are intended as guides to the US states.

Effects of the Molar Ratios of $KMnO_4$ *and* $NaHSO_3$

The effect of the ratio of $KMnO_4$ to $NaHSO_3$ on the oxidation of PAHs in an aqueous solution was examined; the data are plotted in Fig. 1. In these experiments, $KMnO_4$ concentration is fixed, $NaHSO_3$ concentration decreases, and Mn(III) will be generated in a complex series of chemical reactions (Sun et al. 2015, 2016a). To clearly describe the key role of $NaHSO_3$ in AOP, three main chemical reactions were evaluated to interpret experimental observations. Depending on the $NaHSO_3$ concentration, ranging from excess to shortage, permanganate can be reduced to manganese intermediates through one of the following reaction routes, as illustrated in Eqs. (7)–(9)

$$2MnO_4^- + 5HSO_3^- \rightarrow 2Mn^{2+} + 5SO_4^{2-} + OH^- + H_2O \quad (7)$$

$$2MnO_4^- + 4HSO_3^- \rightarrow Mn^{2+} + 4SO_4^{2-} + MnO_2 + 2H_2O \quad (8)$$

$$2MnO_4^- + 3HSO_3^- + H_2O \rightarrow MnO_2 + 3SO_4^{2-} + 2OH^- \quad (9)$$

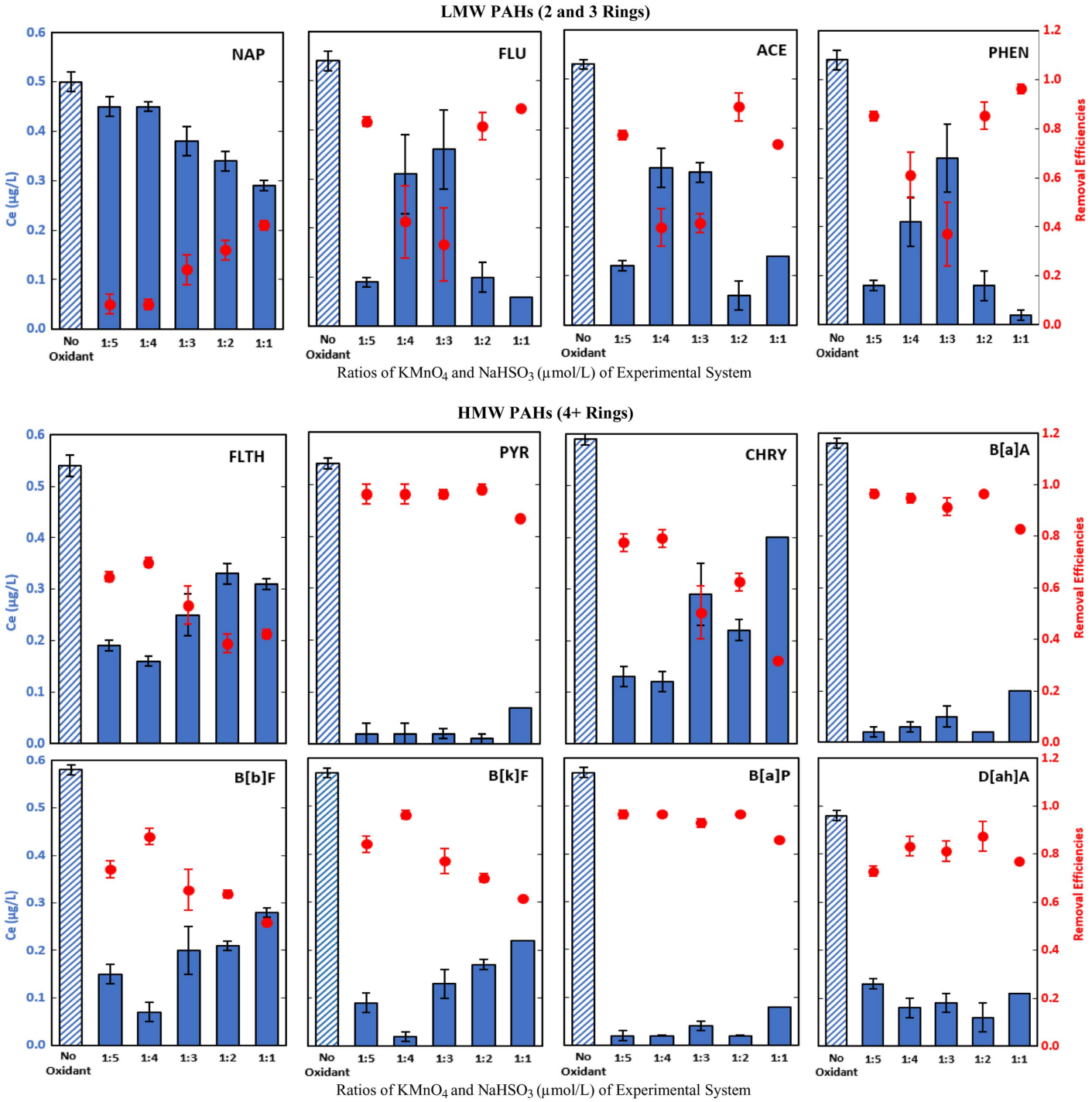

Fig. 1. Final concentrations (bars, left axis) and removal efficiencies (symbols, right axis) of 12 PAHs at varying ratios of $KMnO_4$ and $NaHSO_3$ following $KMnO_4/NaHSO_3$ oxidation in initial $C_{[16PAHs]} = 0.8$ μg/L (0.064 μmol/L) solutions containing 2 mg-OC/L humic acid, pH = 6.5, $C_{[16PAHs]}$:$C_{[KMnO_4]}$ (μmol/L) = 1:30, and RT = 5 min. Error bars represent one standard deviation.

Table 4. Concentrations of MnO_4^-, Mn(II), and SO_4^{2-} at different molar ratios of $KMnO_4$ and $NaHSO_3$

Parameters	$C_{[KMnO_4]}$:$C_{[NaHSO_3]}$ (μmol/L) = 1:1[a]	$C_{[KMnO_4]}$:$C_{[NaHSO_3]}$ (μmol/L) = 1:2	$C_{[KMnO_4]}$:$C_{[NaHSO_3]}$ (μmol/L) = 1:3	$C_{[KMnO_4]}$:$C_{[NaHSO_3]}$ (μmol/L) = 1:4	$C_{[KMnO_4]}$:$C_{[NaHSO_3]}$ (μmol/L) = 1:5
$C_{MnO_4^-}$ (μg/L)	226.95	226.95	226.95	226.95	226.95
Forms of Mn	MnO_4^-, Mn(II), and Mn_xO_y	Mn(II) and Mn_xO_y	Mn(II) and Mn_xO_y	Mn(II)	Mn(II)
Solution characters[b]	Purple with solids	Colorless with solids	Colorless with solids	Colorless and no solid	Colorless and no solid
CMn (II) (μg/L)	9.16 ± 2.06[c]	16.72 ± 1.07	71.50 ± 9.16	99.33 ± 4.73	101.09 ± 7.27
Theoretical CMn (II) (μg/L)	0	52.47	104.94	104.94	104.94
$C_{SO_4^{2-}}$ (μg/L)	—	376.19 ± 6.90	583.83 ± 53.30	717.10 ± 49.67	840.95 ± 4.43
Theoretical $C_{SO_4^{2-}}$ (μg/L)	—	366.34	549.50	732.67	915.84

[a]The experiments were conducted at the condition of $C_{[16PAHs]}$:$C_{[KMnO_4]}$ (μmol/L) = 1:30.
[b]The initial color of PAHs solutions containing 2 mg-OC/L HA is yellowish.
[c]The number after the "±" represents the standard deviation.

AOP Behavior and PAH Oxidation at Excess Bisulfite Concentrations [$C_{[KMnO_4]}$:$C_{[NaHSO_3]}$ (μmol/L) = 1:4 and 1:5]

The C_e values of HMW PAHs, excluding D[ah]A, decreased at high bisulfite concentrations (Fig. 1), and the removal efficiencies of these molecules, excluding FLTH, increased to more than 70%. In contrast, the C_e values of LMW PAHs, excluding NAP, decreased, and the removal efficiencies of these molecules increased. During the experiments, no precipitation was observed after adding $NaHSO_3$ into the solution, and the colorless solution indicated that $KMnO_4$ was completely consumed. It indicated that PAHs only were oxidized by Mn(III) generated in the Mn(VII)/bisulfite AOP, and no flocculation-precipitation occurred. Table 4 shows the concentration of Mn(II) as 99.33 ± 4.7 μg/L in the case of $C_{[KMnO_4]}$:$C_{[NaHSO_3]}$ (μmol/L) = 1:4 and 101.09 ± 7.3 μg/L in the case of $C_{[KMnO_4]}$:$C_{[NaHSO_3]}$ (μmol/L) = 1:5; it indicated that all Mn(VII) reacted to Mn(II). Thus, it is hypothesized that the reaction described in Eq. (7) dominates at $C_{[KMnO_4]}$:$C_{[NaHSO_3]}$ (μmol/L) = 1:4 and 1:5.

AOP Behavior and PAH Oxidation at Midrange Bisulfite Concentrations [$C_{[KMnO_4]}$:$C_{[NaHSO_3]}$ (μmol/L) = 1:2 and 1:3]

At midrange concentrations of $KMnO_4$, the C_e values for HMW PAHs decreased, and the removal efficiencies of these molecules increased, but the C_e values for LMW PAHs, excluding ACE, increased, and the removal efficiencies of these molecules decreased. Under these conditions, the solution was colorless after adding $NaHSO_3$ into the solution, indicating that $KMnO_4$ was completely reacted. While the ratios of $NaHSO_3$ concentration increased, MnO_2 solid was generated rapidly, but the quantities of MnO_2 decreased. Table 4 shows the concentration of Mn(II) as 16.72 ± 1.1 μg/L in the case of $C_{[KMnO_4]}$:$C_{[NaHSO_3]}$ (μmol/L) = 1:2 and 71.50 ± 9.2 μg/L in the case of $C_{[KMnO_4]}$:$C_{[NaHSO_3]}$ (μmol/L) = 1:3, indicating that the increase in Mn(II) corresponds with a decrease in MnO_2. Thus, it is hypothesized that the reaction described in Eq. (8) dominates at $C_{[KMnO_4]}$:$C_{[NaHSO_3]}$ (μmol/L) = 1:2 and 1:3.

Prior research (Sun et al. 2016b) explained the mechanisms of AOP in the removal of phenol from aqueous solution. Firstly, the $KMnO_4$/$NaHSO_3$ reactions occurred in the process of organic contaminants degradation in the aqueous solution and generated H^+. The reactions include

$$2HSO_3^- + MnO_4^- \rightarrow Mn(III) + 2OH^- + 2SO_4^{2-} \quad (10)$$

$$HSO_3^- + 2Mn(III) + H_2O \rightarrow 2Mn^{2+} + 2SO_4^{2-} + 3H^+ \quad (11)$$

$$2Mn(III) + 2H_2O \rightarrow Mn^{2+} + MnO_2 + 4H^+ \quad (12)$$

$$Mn(III) + \text{target compounds} \rightarrow 2Mn^{2+} + \text{products} \quad (13)$$

In total, $7H^+$ and $2OH^-$ were generated. Obviously, the quantities of H^+ is more than those of OH^-. The higher concentration of $NaHSO_3$ could promote reaction efficiency (Sun et al. 2016a). Secondly, MnO_4^- and a small amount of nonoxidizing colloidal MnO_2 were reduced to Mn(II) and manganese intermediates with a sufficient amount of $NaHSO_3$. The main reactive intermediate was Mn(III) in the AOP process. The stabilization time of Mn (III) is very short (i.e., ~10 ms) in the acidic solution (Sun et al. 2016a). The high oxidative chemical activity of Mn(III) can oxidize organic contaminants and generate Mn(II). It was found out that benzene, which could not be oxidized by permanganate even at high temperatures (Waldemer and Tratnyek 2006), could be rapidly transformed to phenol in the AOP process (Sun et al. 2016a). The excessive Mn(III) could be the generation of Mn(II) and MnO_2 because of Mn(III) disproportionation, which is a side effect of the Mn(III) oxidation reaction, as reported in the previous study (Sun et al. 2015). Meanwhile, the nonoxidizing colloidal MnO_2 could be transformed to the in situ formed MnO_2, a strong oxidizing agent, under acidic conditions, and this phenomenon was reported in the previous study (Sun et al. 2016b). Under neutral or alkaline conditions, nonoxidizing colloidal MnO_2 potentially adsorbed contaminants and precipitated together. It is hypothesized that flocculation-precipitation is a potential PAH removal factor when a lot of MnO_2 exists. Even though these studies were performed on single-ringed aromatic structures, these principles might also apply to the treatment of PAHs.

AOP Behavior and PAH Oxidation at Insufficient Bisulfite Concentrations [$C_{[KMnO_4]}$:$C_{[NaHSO_3]}$ (μmol/L) = 1:1]

At concentration ratios $C_{[KMnO_4]}$:$C_{[NaHSO_3]}$ (μmol/L) = 1:1, C_e values for some of HMW PAH (including PYR, B[a]A, B[a]P, and D[ah]A) were low, and the removal efficiencies of these molecules were high. However, C_e values for other HMW PAHs (FLTH, CHRY, B[b]F, and B[K]F) and LMW PAHs were high (and the removal efficiencies were low). During the experiments, it was observed that the color of aqueous solutions remained purple even after the $NaHSO_3$ addition, which indicated that $KMnO_4$ was excessive, and MnO_2 solids were generated rapidly during the reaction. A small quantity of Mn(III) must be generated in the Mn(VII)/bisulfite AOP while $KMnO_4$ and $NaHSO_3$ react, but the excessive $KMnO_4$ cannot further oxidize PAHs. In addition, prior research has reported that a large amount of nonoxidizing colloidal MnO_2 can be generated when the amount of $NaHSO_3$ is insufficient, and these colloidal MnO_2 molecules promoted contaminant adsorption (Sun et al. 2016b). This indicates that the Mn(VII)/bisulfite AOP generated insufficient Mn(III) to oxidize PAHs at this ratio, and some PAHs were potentially adsorbed on colloidal MnO_2 to remove via a process mimicking flocculation-precipitation

simultaneously, but Fig. 1 does not distinguish between different removal mechanisms. Thus, it is hypothesized that the reaction described in Eq. (9) dominates at $C_{[KMnO_4]}$:$C_{[NaHSO_3]}$ (μmol/L) = 1:1. Table 4 shows the concentration of Mn(II) as 9.16 ± 2.0 μg/L.

For $C_{[KMnO_4]}$:$C_{[NaHSO_3]}$ (μmol/L) = 1:5 to 1:1, the C_e of B[a]P was slightly increased from 0.02 to 0.08 μg/L, and the SO_4^{2-} concentrations ranged from 840.95 ± 4.43 to 376.19 ± 6.90 μg/L at $C_{[KMnO_4]}$:$C_{[NaHSO_3]}$ (μmol/L) = 1:5 to 1:2, as shown in Table 4. All MnO_4^- was reduced to Mn(II) by the excessive HSO_3^-, and the residual HSO_3^- was oxidized to sulfate by O_2 under these conditions. Because $C_{[KMnO_4]}$:$C_{[NaHSO_3]}$ (μmol/L) = 1:4 and 1:2, different reaction mechanisms occurred at the reactant ratio, and the effects of the reaction time at both ratios were investigated in the effect of RT experiments.

Effects of the Molar Ratios of PAHs and $KMnO_4$

Fig. 2 shows that the removal efficiencies for HMW PAHs generally increased as concentrations of the oxidant $KMnO_4$ increased relative to the concentration of PAHs, and the greatest removal efficiency was at the molar ratio ($C_{[16PAHs]}$:$C_{[KMnO_4]}$) = 1:50. The C_e values of CHRY, B[b]F, B[k]F, and D[ah]A were most notably decreased under this condition. The C_e values of LMW PAHs fluctuated inconsistently as the molar ratio $C_{[16PAHs]}$:$C_{[KMnO_4]}$ increased.

For $C_{[16PAHs]}$:$C_{[KMnO_4]}$ (μmol/L) = 1:50 to 1:10 and the presence of excess sulfite, the C_e of B[a]P slightly increased from ND to 0.06 μg/L and was still lower than 0.2 μg/L. The removal efficiency of B[a]P was consistent with a previous study, which showed that a relative reactivity order of oxidized PAHs: B[a]P > PYR > FLTH > CHRY (Brown et al. 2003). Brown et al. (2003) studied $KMnO_4$ oxidation of PAHs but used bisulfite as a reaction quencher, which may have inadvertently promoted the AOP process described in this study.

One particular concern with manganese oxidation in surface water systems is the residual Mn(II). As shown in Table 4, Mn(II) concentrations ranged from 101.09 ± 7.3 to 9.16 ± 2.0 μg/L at $C_{[16PAHs]}$:$C_{[KMnO_4]}$ = (μmol/L) 1:50 to 1:10. Subsequent experiments utilized $C_{[16PAHs]}$:$C_{[KMnO_4]}$ (μmol/L) = 1:30, which provides a sufficient removal rate efficiency while ensuring residual Mn(II) concentrations remain below the SMCL.

Control of Mn(II) and Sulfate Concentrations

Theoretically, Mn(II) [assuming the Mn(II) produced is entirely soluble] and sulfate concentrations would be 0.107 mg/L and 732.3 μg/L in the case of the initial $C_{[16PAHs]} = 0.8$ μg/L (0.064 μmol/L) and $C_{[16PAHs]}$:$C_{[KMnO_4]}$:$C_{[NaHSO_3]}$ (μmol/L) = 1:30:120. The Mn(II) concentrations are difficult to predict when MnO_2 precipitation is expected, such as the case of the initial $C_{[16PAHs]} = 0.8$ μg/L and $C_{[16PAHs]}$:$C_{[KMnO_4]}$:$C_{[NaHSO_3]}$ (μmol/L) = 1:30:60, but the sulfate concentration under these conditions would be approximately 366.3 μg/L.

Our experiments results showed 0.099 ± 0.004 mg/L Mn(II) and 717.10 ± 49.67 μg/L sulfate in the case of initial $C_{[16PAHs]} = 0.8$ μg/L and $C_{[16PAHs]}$:$C_{[KMnO_4]}$:$C_{[NaHSO_3]}$ (μmol/L) = 1:30:120. All MnO_4^- was reduced to Mn(II) by the excessive HSO_3^- and the residual HSO_3^- was oxidized to sulfate by O_2 under these conditions. Thus, the actual Mn(II) and sulfate concentrations were consistent with the theoretical values of Mn(II) and sulfate concentrations. Mn(II) was twice higher than Mn(II) SMLC, and the sulfate was below the proposed value in NSDWRs.

For the case of initial $C_{[16PAHs]} = 0.8$ μg/L and $C_{[16PAHs]}$:$C_{[KMnO_4]}$:$C_{[NaHSO_3]}$ (μmol/L) = 1:30:60, the final Mn(II) and sulfate concentrations were 0.016 ± 0.001 mg/L and 376.19 ± 6.90 μg/L, respectively. A large amount of MnO_4^- was reduced to the precipitation, and only a small amount of MnO_4^- was converted to Mn(II) from HSO_3^-, but the sulfate was conserved. In this scenario, detected Mn(II) was significantly lower than SMCL in NSDWRs. If sufficient time is available, the case of $C_{[16PAHs]}$:$C_{[KMnO_4]}$:$C_{[NaHSO_3]}$ (μmol/L) = 1:30:60 [$m_{[16PAHs]}$:$m_{[KMnO_4]}$:$m_{[NaHSO_3]}$ (μg/L) = 1:22:29] and RT = 30 min is recommended, as these conditions minimize residual Mn(II) and sulfate in the aqueous solution. For time-critical or an emergency scenario, $C_{[16PAHs]}$:$C_{[KMnO_4]}$:$C_{[NaHSO_3]}$ (μmol/L) = 1:30:120 [$m_{[16PAHs]}$:$m_{[KMnO_4]}$:$m_{[NaHSO_3]}$ (μg/L) = 1:22:58] and RT = 5 min is recommended, but Mn(II) concentration will exceed the SMCL.

Effect of Reaction Time

Results from reaction time experiments are shown in Fig. 3. As shown in Fig. 3, although RTs were extended from 0.5 to 30 min at $C_{[16PAHs]}$:$C_{[KMnO_4]}$:$C_{[NaHSO_3]}$ (μmol/L) = 1:30:120, the C_e values of HMW PAHs were mostly stable across the reaction times assessed, and the removal efficiencies of these molecules, excluding CHRY and D[ah]A, exceeded 90%. In contrast, C_e values and the removal efficiencies of LMW PAHs, excluding NAP, fluctuated inconsistently. A prior study showed that benzene, aniline, and bisphenol A oxidation using Mn(VII)/bisulfite at $C_{[contaminants]}$:$C_{[KMnO_4]}$:$C_{[NaHSO_3]}$ (μmol/L) = 1:20:200 was completed in 1 s (Sun et al. 2016a). In this study, HMW PAHs were also oxidized rapidly in 5 min. Also, no MnO_2 was retained during filtration. For RTs = 0.5–30 min at $C_{[16PAHs]}$:$C_{[KMnO_4]}$:$C_{[NaHSO_3]}$ (μmol/L) = 1:30:120, C_e of B[a]P was changed slightly from ND to 0.02 μg/L.

Results differ slightly for the case of $C_{[16PAHs]}$:$C_{[KMnO_4]}$:$C_{[NaHSO_3]}$ (μmol/L) = 1:30:60 (Fig. 4) compared to the case of $C_{[16PAHs]}$:$C_{[KMnO_4]}$:$C_{[NaHSO_3]}$ (μmol/L) = 1:30:120 (Fig. 3). Fig. 4 showed that the C_e values of LMW PAHs (FLU, ACE, and PHEN) were low at 1 and 5 min and increased at 10 min, but there was no obvious change in C_e values after 10 min. In contrast, C_e values of HMW PAHs (CHRY, B[b]F, B[k]F, and D[ah]A) gradually decreased from 1 to 10 min and remained at low concentrations after 10 min. The trends of C_e values of PYR, B[a]A, and B[b]F were below detection limits after 1 min. Mn(III) oxidation proceeds rapidly and can completely react in a very short time; however, PAH removal was most completed when the reaction time exceeds 10 min or more. This suggests a secondary removal mechanism, such as the adsorption and precipitation processes hypothesized in the section "Effects of the Molar Ratios of $KMnO_4$ and $NaHSO_3$." The removal efficiencies of PAHs at 10 min were better than the 5 min experiments described in the section "Effects of the Molar Ratios of $KMnO_4$ and $NaHSO_3$." This time dependency proves strong evidence in support of the adsorption and precipitation hypothesis, but further experiments are needed to justify the hypotheses fully. In addition, when $C_{[16PAHs]}$:$C_{[KMnO_4]}$:$C_{[NaHSO_3]}$ (μmol/L) = 1:30:60, the C_e of B[a]P was still less than 0.02 μg/L.

Effect of the pH

The extent of PAH oxidation as a function of the pH was investigated using pH values ranging from 5.0 to 8.0, which is loosely based on pH values observed in the Neches River (Beaumont, Texas) between 2014 and 2016 (TCEQ 2017). The C_e and removal efficiencies of the PAH compounds investigated are shown in Fig. 5.

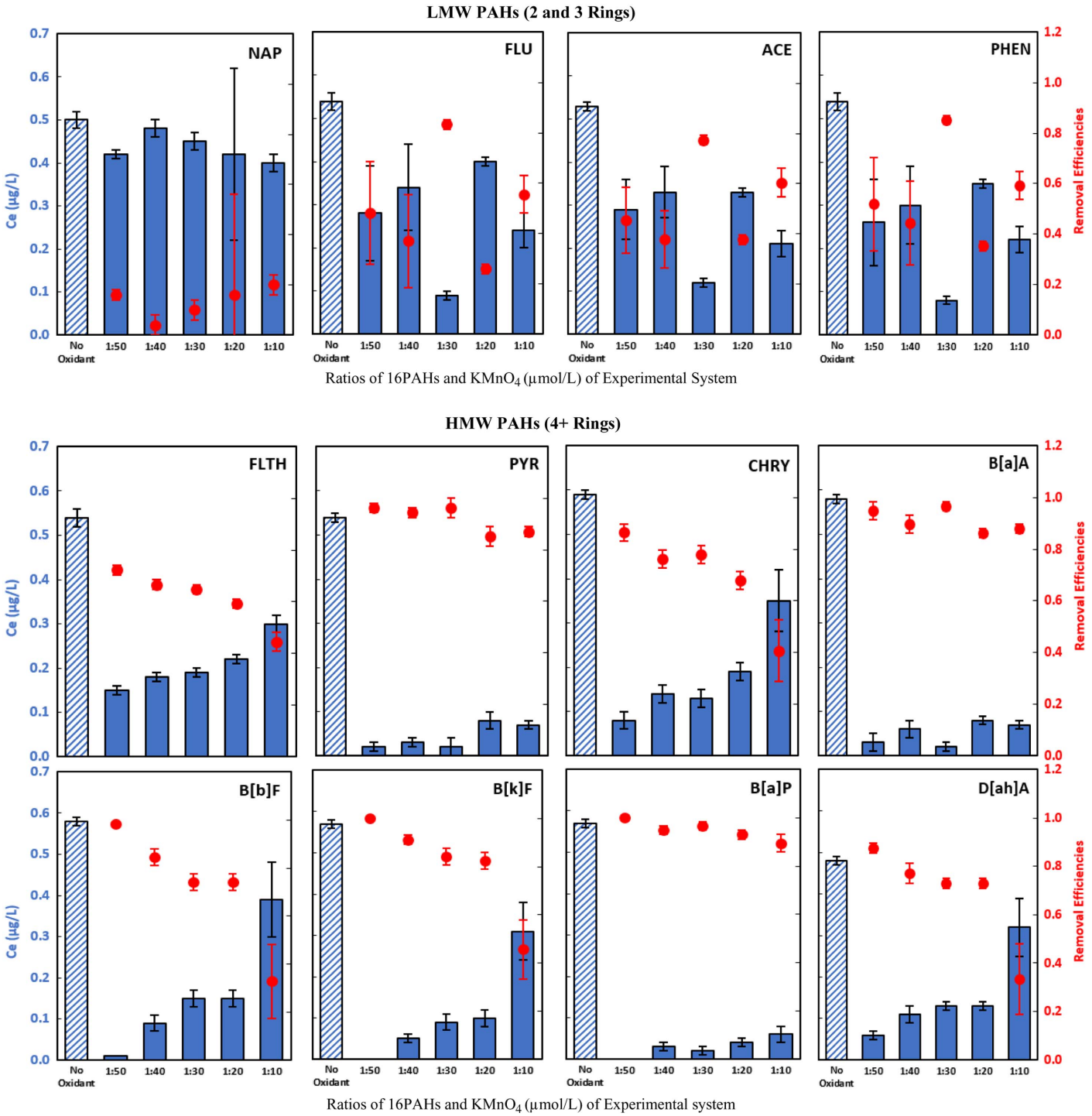

Fig. 2. Final concentrations (bars, left axis) and removal efficiencies (symbols, right axis) of 12 PAHs at varying ratios of 16PAHs and $KMnO_4$ following $KMnO_4/NaHSO_3$ oxidation in initial $C_{[16PAHs]} = 0.8$ μg/L (0.064 μmol/L) solutions containing 2 mg-OC/L humic acid, pH = 6.5, $C_{[KMnO_4]}$:$C_{[NaHSO_3]}$ (μmol/L) = 1:5, and RT = 5 min. Error bars represent one standard deviation.

In general, the removal efficiencies decreased with an increasing pH, with the lowest removal efficiencies obtained at pH 7.95. The results correspond to those of previous studies (Xiao et al. 2013) that acid-catalysis of $KMnO_4/NaHSO_3$ oxidation promoted the generation of highly active Mn(III) to remove over 99% ciprofloxacin at a pH of 4.5, while the removal of ciprofloxacin dropped progressively as the pH increased from 7.0 to 9.0. However, for HMW PAHs, such as B[b]F, B[a]P, and B[k]F, PAH REs approached 100%; for instance, for all pH values assessed, the C_e of B[a]P was very close to ND μg/L.

The effect of the pH was most pronounced for HMW PAHs. In general, the C_e of LMW PAHs were high, and the removal efficiencies of these molecules were insignificant. However, like the screening experiment, the removal efficiencies of all HMW PAHs exceeded 80% (excluding FLTH, whose was closer to 70%) for all pH conditions tested, much higher than those obtained for

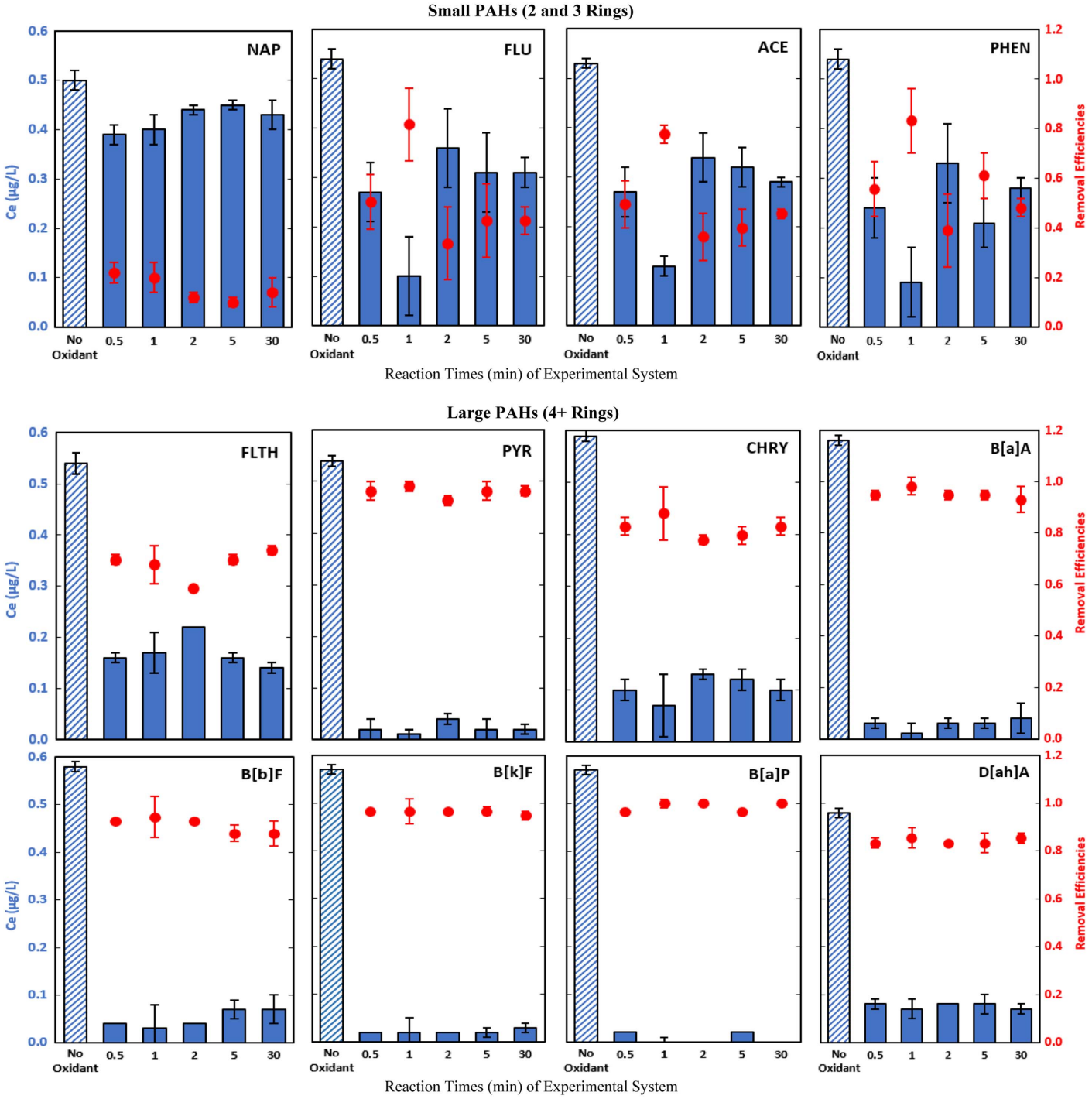

Fig. 3. Final concentrations (bars, left axis) and removal efficiencies (symbols, right axis) of 12 PAHs at varying reaction times following $KMnO_4/NaHSO_3$ oxidation in initial $C_{[16PAHs]} = 0.8\ \mu g/L$ (0.064 μmol/L) solutions containing 2 mg-OC/L humic acid, pH = 6.5, and $C_{[16PAHs]}$:$C_{[KMnO_4]}$:$C_{[NaHSO_3]}$ (μmol/L) = 1:30:120. Error bars represent one standard deviation.

LMW PAHs. This suggests that Mn(VII)/bisulfite AOP primarily oxidizes HMW PAHs in a wide range of pH. The reason may be that HMW PAHs could be converted into small organic molecules by permanganate when H^+ exists. As pH did not significantly affect the extent of oxidation for most PAH compounds, the pH = 6.5 (pH of D.I. water and consistent with many surface water bodies) was used in the subsequent optimal experiments.

As observed in the screening experiment, removal efficiencies of ANTH were always 100%, regardless of the pH and other AOP parameters, as shown in Fig. 6. Cavalieri and Rogan (1990) reported that one-electron oxidation produced PAH radical cations and PAH (anthracene) with ionization potentials below ca. 7.35 eV, which can be activated by one-electron oxidation. In addition, Lee et al. (1998) reported that about 80% of 9,10-anthraquinone was generated when 97% of ANTH was oxidized using the Fenton treatment. The oxidation performance of Mn(VII)/bisulfite AOP is stronger than the Fenton, which suggests that ANTH can be completely oxidized using this AOP, as our data suggest. However, the

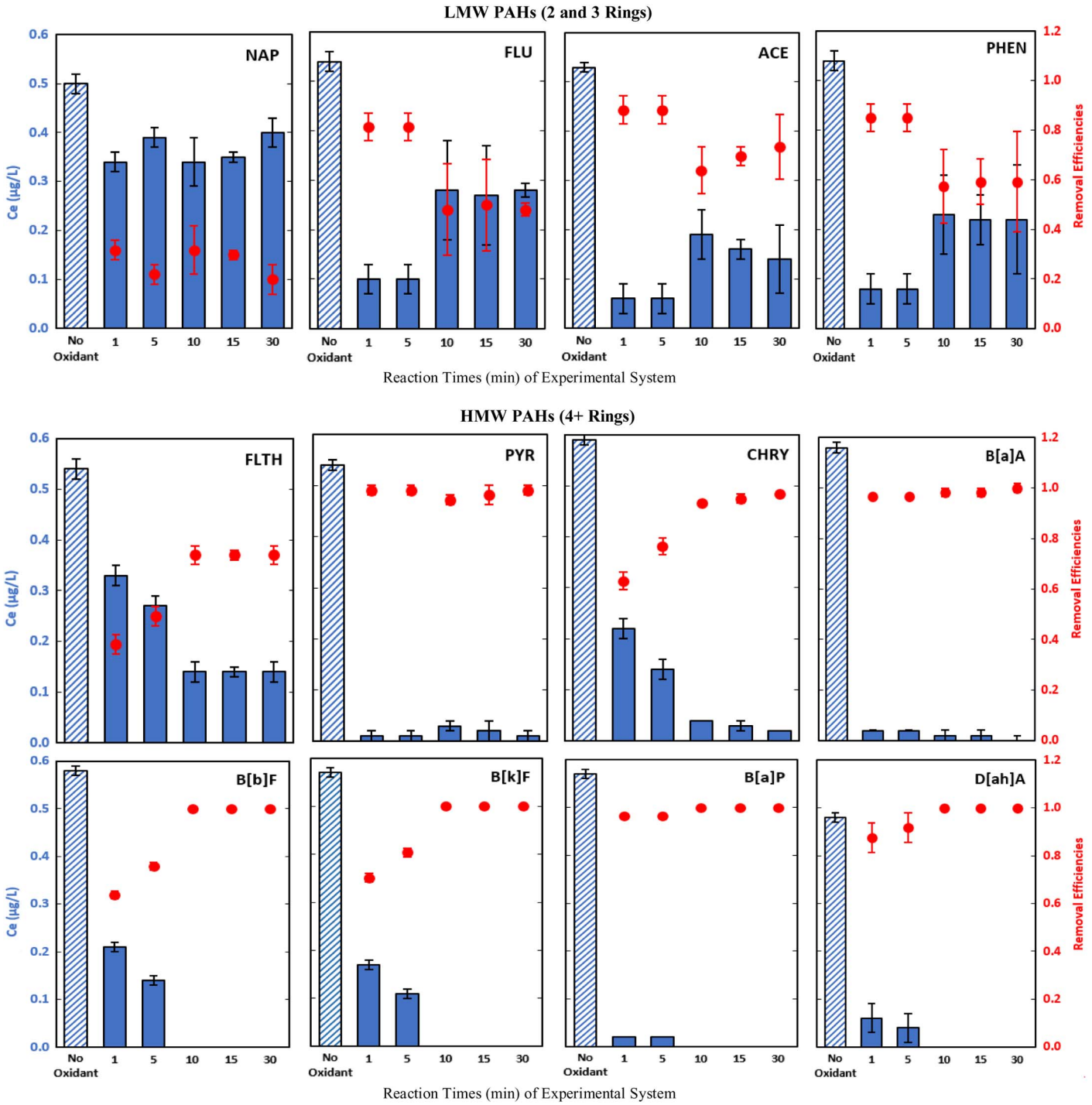

Fig. 4. Final concentrations (bars, left axis) and removal efficiencies (symbols, right axis) of 12 PAHs at varying reaction times following $KMnO_4/NaHSO_3$ oxidation in initial $C_{[16PAHs]} = 0.8$ μg/L (0.064 μmol/L) solutions containing 2 mg-OC/L humic acid, pH = 6.5, and $C_{[16PAHs]}$:$C_{[KMnO_4]}$:$C_{[NaHSO_3]}$ (μmol/L) = 1:30:60. Error bars represent one standard deviation.

mechanism of the degradation of ANTH needs more data and experiments to interpret.

Effect of HA

Results from the initial screening experiment were shown in Fig. 7. The HA appeared to have a minimal effect on the extent of the PAH oxidation. The differences in residual concentration of each PAH compound in experiments with and without HA were less than 5% and determined to be negligible. Sun et al. (2013) reported that the reductive properties of HA promote the oxidation of phenol by permanganate along at pH < 7.0 but are less reactive at pH > 7.0, which was very different from the results we obtained with HA. During our experiments, experimental solutions containing HA and PAHs were initially yellowish in color but became colorless after amendment with Mn(VII)/bisulfite, indicating that HA molecules were oxidized. This suggests that PAH molecules originally adsorbed on HA molecules reentered the water phase and then were

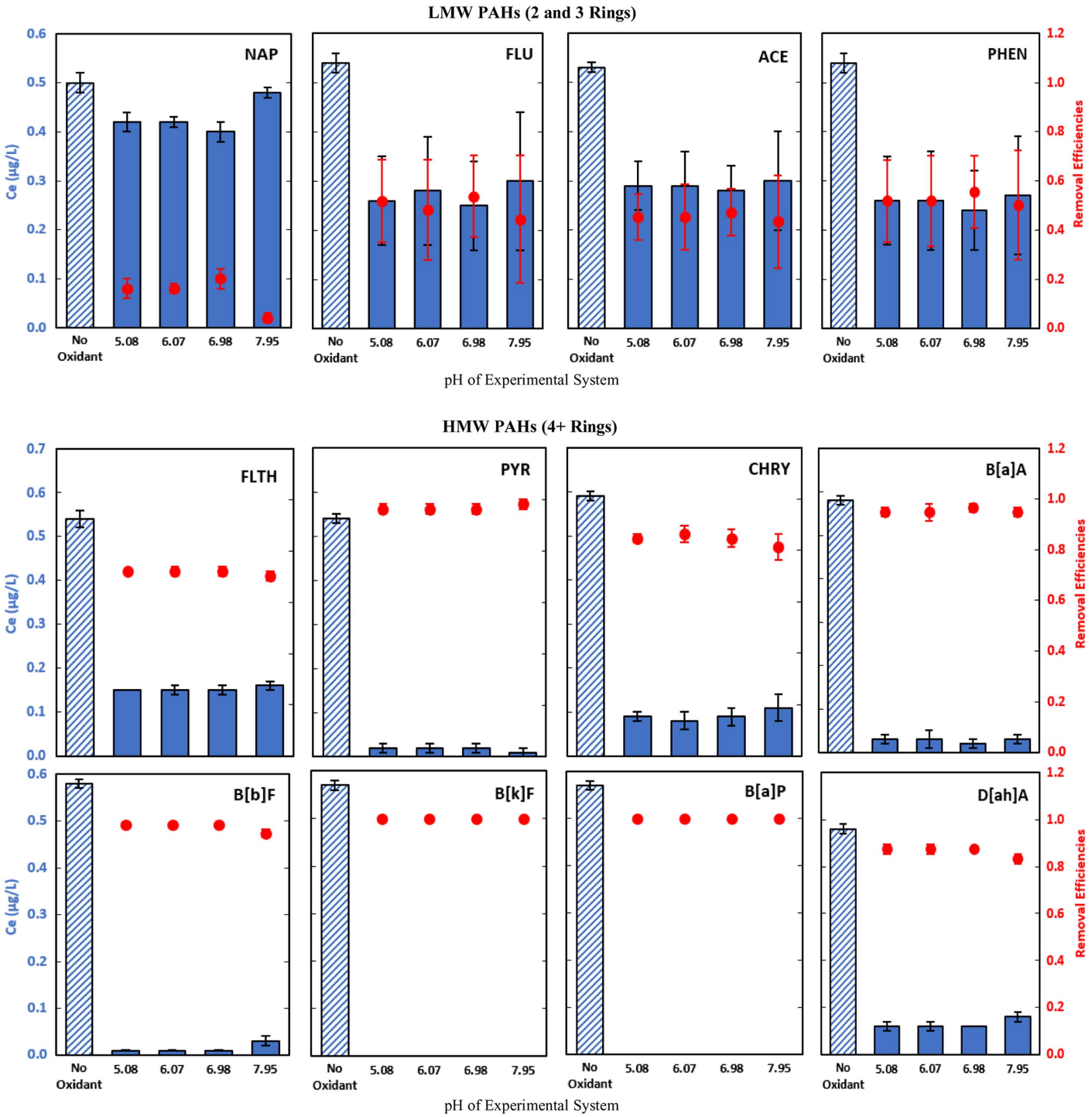

Fig. 5. Final concentrations (bars, left axis) and removal efficiencies (symbols, right axis) of 12 PAHs at varying initial pH values following $KMnO_4/NaHSO_3$ oxidation in initial $C_{[16PAHs]} = 0.8$ μg/L (0.064 μmol/L) solutions containing 2 mg-OC/L humic acid, $C_{[16PAHs]}$:$C_{[KMnO_4]}$:$C_{[NaHSO_3]}$ (μmol/L) = 1:50:250, and RT = 5 min. Error bars represent one standard deviation.

oxidized or were directly oxidized in the organic phase by Mn(VII)/bisulfite. Overall, our data indicated that the proposed Mn(VII)/bisulfite AOP was highly effective for HMW PAHs at the conditions tested [pH = 7.0, $C_{[16PAHs]}$:$C_{[KMnO_4]}$:$C_{[NaHSO_3]}$ (μmol/L) = 1:50:250, and RT = 5 min] with and without HA. Based on these data, all subsequent optimal experiments were conducted with 2 mg-OC/L, as this is a representative organic carbon content for surface water.

The results also showed that the residual fractions (C_e/C_0) of LMW PAHs postoxidation were high, and the removal efficiencies of these molecules were insignificant. However, the removal efficiencies of HMW PAHs were greater than 80% (excluding FLTH), which is much higher than the removal efficiencies obtained for LMW PAHs in solutions containing either 0 or 2 mg-OC/L HA. This is consistent with the observations of Brown et al. (2003) and Forsey et al. (2010), who also showed that HMW PAHs were

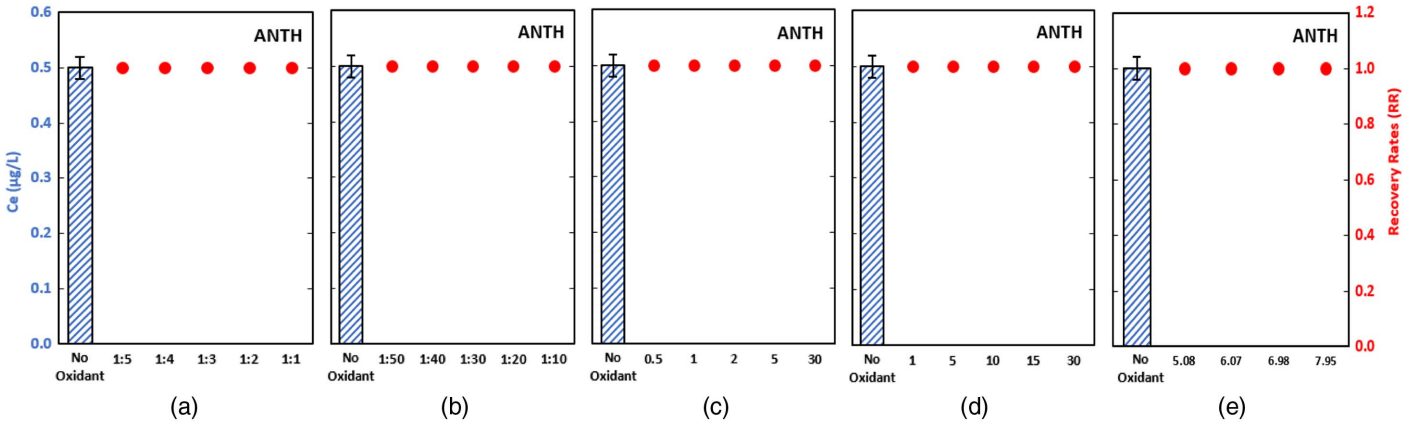

Fig. 6. Final concentrations (bars, left axis) and removal efficiencies (symbols, right axis) of ANTH at the optimized $KMnO_4/NaHSO_3$ oxidation of (a–e). Error bars represent one standard deviation: (a) ratios of $KMnO_4$ and $NaHSO_3$ of experimental system in the initial $C_{[16PAHs]} = 0.8\ \mu g/L$ (0.064 μmol/L) solutions containing 2 mg-OC/L humic acid, pH = 6.5, $C_{[16PAHs]}:C_{[KMnO_4]}$ (μmol/L) = 1:30, and reaction time = 5 min; (b) ratios of 16PAHs and $KMnO_4$ of experimental system in initial $C_{[16PAHs]} = 0.8\ \mu g/L$ (0.064 μmol/L) solutions containing 2 mg-OC/L humic acid, pH = 6.5, $C_{[KMnO_4]}:C_{[NaHSO_3]}$ (μmol/L) = 1:5, and reaction time = 5 min; (c) reaction times of experimental system in initial $C_{[16PAHs]} = 0.8\ \mu g/L$ (0.064 μmol/L) solutions containing 2 mg-OC/L humic acid, pH = 6.5, and $C_{[16PAHs]}:C_{[KMnO_4]}:C_{[NaHSO_3]}$ (μmol/L) = 1:30:120; (d) reaction times of experimental system in initial $C_{[16PAHs]} = 0.8\ \mu g/L$ (0.064 μmol/L) solutions containing 2 mg-OC/L humic acid, pH = 6.5, and $C_{[16PAHs]}:C_{[KMnO_4]}:C_{[NaHSO_3]}$ (μmol/L) = 1:30:60; and (e) pH of experimental system in initial $C_{[16PAHs]} = 0.8\ \mu g/L$ (0.064 μmol/L) solutions containing 2 mg-OC/L humic acid, $C_{[16PAHs]}:C_{[KMnO_4]}:C_{[NaHSO_3]}$ (μmol/L) = 1:50:250, and reaction time = 5 min.

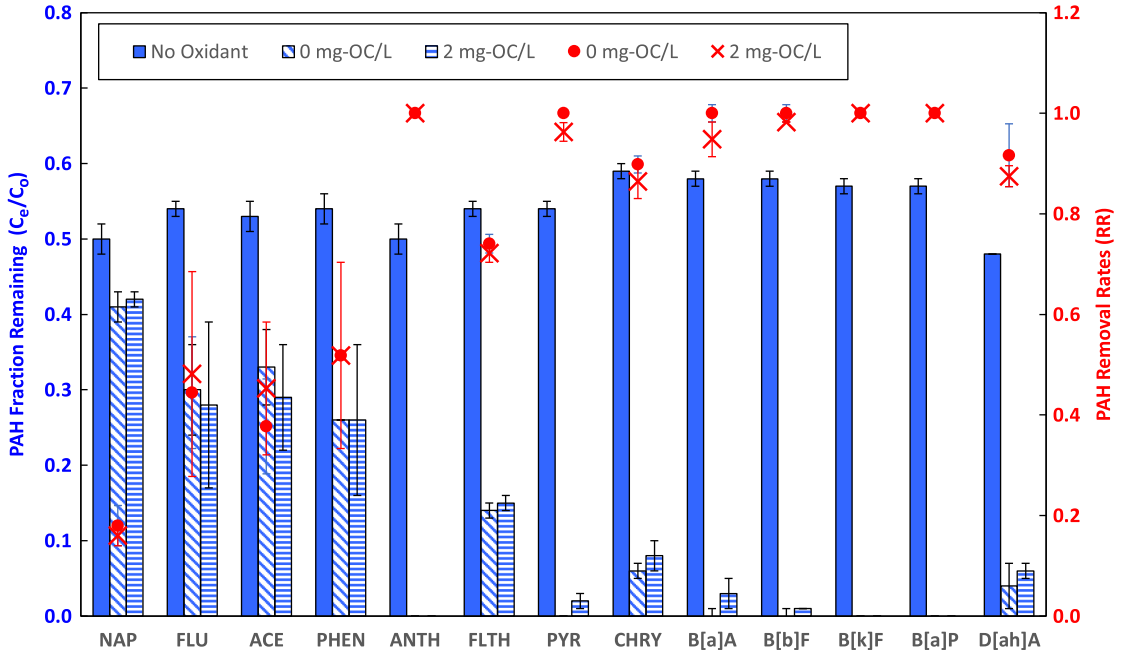

Fig. 7. Residual fraction (bars, left axis) and removal efficiencies (symbols, right axis) of 13 PAHs following $KMnO_4/NaHSO_3$ oxidation in solutions containing 0 and 2 mg-OC/L of humic acid. Error bars represent one standard deviation.

subject to much greater degrees of oxidation by permanganate than LMW PAHs.

Conclusions

Advanced oxidation using permanganate and bisulfite is an effective method to remove HMW PAHs, but it is unable to remove LMW PAHs completely. The dosage ratio of permanganate and bisulfite needs to be carefully controlled to avoid the generation of by-products and minimize treatment costs. Optimal operational conditions identified in this study using D.I. water and 2 mg-OC/L HA were $C_{[16PAHs]}:C_{[KMnO_4]}:C_{[NaHSO_3]}$ (μmol/L) = 1:30:60 [$m_{[16PAHs]}:m_{[KMnO_4]}:m_{[NaHSO_3]}$ (μg/L) = 1:22:29] and RT = 30 min, which effectively oxidized HMW PAHs over a wide pH range (5.0–8.0). After being treated by Mn(VII)/bisulfite for 30 min, the B[a]P concentration was below MCL of 0.2 μg/L. This demonstrated that AOP treatment is much faster than GAC adsorption (which can take up to 24 h). Under these conditions, final Mn(II) concentration in water was less than

0.05 mg/L, while sulfate concentrations were much less than 250 mg/L. If the dosages of $KMnO_4$ and $NaHSO_3$ are controlled well, Mn(VII)/bisulfite AOP has the potential to be a relatively safe technology for remediating PAH in water.

Data Availability Statement

Some or all data, models, or codes that support the findings of this study are available from the corresponding author upon reasonable request.

Acknowledgments

This work has been financially supported by the National Science Foundation (LU#1760710 and TTU#1760673), the Texas Hazardous Waste Research Center (118LUB0058H and 110LUB0075H), and the Maddox Engineering Research Center Labs at Texas Tech University. We also thank Professor Andrew Jackson of Texas Tech University for providing the sulfate analysis.

References

Abdullah, N., H. A. Aziz, N. N. A. N. Yusuf, M. Umar, and S. S. A. Amr. 2014. "Potential of KMnO4 and H2O2 in treating semi-aerobic landfill leachate." *Appl. Water Sci.* 4 (3): 303–309. https://doi.org/10.1007/s13201-013-0146-6.

Abernathy, C., D. Cole, M. Cassidy, M. Morris, G. Gomez, and L. Lacker. 2003. *Drinking water advisory: Consumer acceptability advice and health effects analysis*. Washington, DC: EPA.

Amadeo, K. 2019. "Hurricane Harvey facts, damage and costs." Accessed September 23, 2019. https://www.thebalance.com/hurricane-harvey-facts-damage-costs-4150087.

Anipsitakis, G. P., D. D. Dionysiou, and M. A. Gonzalez. 2006. "Cobalt-mediated activation of peroxymonosulfate and sulfate radical attack on phenolic compounds. Implications of chloride ions." *Environ. Sci. Technol.* 40 (3): 1000–1007. https://doi.org/10.1021/es050634b.

Ates, H., and M. E. Argun. 2018. "Removal of PAHs from leachate using a combination of chemical precipitation and Fenton and ozone oxidation." *Water Sci. Technol.* 78 (5): 1064–1070. https://doi.org/10.2166/wst.2018.378.

Brown, G. S., L. L. Barton, and B. M. Thomson. 2003. "Permanganate oxidation of sorbed polycyclic aromatic hydrocarbons." *Waste Manage.* 23 (8): 737–740. https://doi.org/10.1016/S0956-053X(02)00119-8.

Cavalieri, E. L., and E. G. Rogan. 1990. "Radical cations in aromatic hydrocarbon carcinogenesis." *Free Radical Res.* 11 (1–3): 77–87. https://doi.org/10.3109/10715769009109670.

Chowdhury, A. N., M. S. Azam, M. Aktaruzzaman, and A. Rahim. 2009. "Oxidative and antibacterial activity of Mn_3O_4." *J. Hazard. Mater.* 172 (2–3): 1229–1235. https://doi.org/10.1016/j.jhazmat.2009.07.129.

Deborde, M., and U. von Gunten. 2008. "Reactions of chlorine with inorganic and organic compounds during water treatment-Kinetics and mechanisms: A critical review." *Water Res.* 42 (1–2): 13–51. https://doi.org/10.1016/j.watres.2007.07.025.

DHHS (Department of Health & Human Services). 1999. "Toxicological profile for polycyclic aromatic hydrocarbons." *J. Toxicol. Cutaneous Ocul. Toxicol.* 18 (2): 141–147. https://doi.org/10.3109/15569529909037564.

EPA. 1986. *Method 8310 polynuclear aromatic hydrocarbons*. Washington, DC: EPA.

EPA. 1994. *Method 200.8 determination of trace elements in waters and wastes by inductively coupled plasma-mass spectrometry environmental monitoring systems laboratory office of research and development U*. Washington, DC: EPA.

EPA. 2012. *US EPA volatile organic chemicals (VOCs) synthetic organic chemicals (SOCs)*. Washington, DC: National Secondary Drinking Water Standards.

Forsey, S. P., N. R. Thomson, and J. F. Barker. 2010. "Oxidation kinetics of polycyclic aromatic hydrocarbons by permanganate." *Chemosphere* 79 (6): 628–636. https://doi.org/10.1016/j.chemosphere.2010.02.027.

Hoigné, J., and H. Bader. 1994. "Kinetics of reactions of chlorine dioxide (OCIO) in water. I: Rate constants for inorganic and organic compounds." *Water Res.* 28 (1): 45–55. https://doi.org/10.1016/0043-1354(94)90118-X.

Hu, L., H. M. Martin, and T. J. Strathmann. 2010. "Oxidation kinetics of antibiotics during water treatment with potassium permanganate." *Environ. Sci. Technol.* 44 (16): 6416–6422. https://doi.org/10.1021/es101331j.

Huber, M. M., S. Korhonen, T. A. Ternes, and U. von Gunten. 2005. "Oxidation of pharmaceuticals during water treatment with chlorine dioxide." *Water Res.* 39 (15): 3607–3617. https://doi.org/10.1016/j.watres.2005.05.040.

Jiang, J., S. Y. Pang, J. Ma, and H. Liu. 2012. "Oxidation of phenolic endocrine disrupting chemicals by potassium permanganate in synthetic and real waters." *Environ. Sci. Technol.* 46 (3): 1774–1781. https://doi.org/10.1021/es2035587.

Kao, C. M., K. D. Huang, J. Y. Wang, T. Y. Chen, and H. Y. Chien. 2008. "Application of potassium permanganate as an oxidant for in situ oxidation of trichloroethylene-contaminated groundwater: A laboratory and kinetics study." *J. Hazard. Mater.* 153 (3): 919–927. https://doi.org/10.1016/j.jhazmat.2007.09.116.

Kochany, J., and E. Lipczynska-Kochany. 1992. "Application of the EPR spin-trapping technique for the investigation of the reactions of carbonate, bicarbonate, and phosphate anions with hydroxyl radicals generated by the photolysis of H_2O_2." *Chemosphere* 25 (12): 1769–1782. https://doi.org/10.1016/0045-6535(92)90018-M.

Lee, B. D., M. Hosomi, and A. Murakami. 1998. "Fenton oxidation with ethanol to degrade anthracene into biodegradable 9, 10-anthraquinon: A pretreatment method for anthracene-contaminated soil." *Water Sci. Technol.* 38 (7 pt 6): 91–97. https://doi.org/10.2166/wst.1998.0281.

Li, R., P. Hua, J. Zhang, and P. Krebs. 2019. "A decline in the concentration of PAHs in Elbe River suspended sediments in response to a source change." *Sci. Total Environ.* 663 (May): 438–446. https://doi.org/10.1016/j.scitotenv.2019.01.355.

Liao, X., Z. Wu, Y. Li, H. Cao, and C. Su. 2019. "Effect of various chemical oxidation reagents on soil indigenous microbial diversity in remediation of soil contaminated by PAHs." *Chemosphere* 226 (Jul): 483–491. https://doi.org/10.1016/j.chemosphere.2019.03.126.

Mojiri, A., J. L. Zhou, A. Ohashi, N. Ozaki, and T. Kindaichi. 2019. "Comprehensive review of polycyclic aromatic hydrocarbons in water sources, their effects and treatments." *Sci. Total Environ.* 696 (Dec): 133971. https://doi.org/10.1016/j.scitotenv.2019.133971.

National Center for Biotechnology Information. 2019. "Explore chemistry." Accessed June 10, 2019. https://pubchem.ncbi.nlm.nih.gov/.

Perez-Benito, J. F. 2011. "Permanganate oxidation of α-amino acids: Kinetic correlations for the nonautocatalytic and autocatalytic reaction pathways." *J. Phys. Chem. A* 115 (35): 9876–9885. https://doi.org/10.1021/jp2043174.

Perez-Benito, J. F., C. Arias, and E. Amat. 1996. "A kinetic study of the reduction of colloidal manganese dioxide by oxalic acid." *J. Colloid Interface Sci.* 177 (2): 288–297. https://doi.org/10.1006/jcis.1996.0034.

Pfaff, J. D. 1993. *Method 300.0 determination of inorganic anions by ion chromatography environmental monitoring systems laboratory office of research and development*. Cincinnati: USEPA.

Qu, C., S. Albanese, A. Lima, D. Hope, P. Pond, A. Fortelli, N. Romano, P. Cerino, A. Pizzolante, and B. De Vivo. 2019. "The occurrence of OCPs, PCBs, and PAHs in the soil, air, and bulk deposition of the Naples metropolitan area, southern Italy: Implications for sources and environmental processes." *Environ. Int.* 124 (Dec): 89–97. https://doi.org/10.1016/j.envint.2018.12.031.

Sun, B., H. Dong, D. He, D. Rao, and X. Guan. 2016a. "Modeling the kinetics of contaminants oxidation and the generation of Mn(III) in the permanganate/bisulfite process." *Environ. Sci. Technol.* 50 (3): 1473–1482. https://doi.org/10.1021/acs.est.5b05207.

Sun, B., X. Guan, J. Fang, and P. G. Tratnyek. 2015. "Activation of manganese oxidants with bisulfite for enhanced oxidation of organic

contaminants: The involvement of Mn(III)." *Environ. Sci. Technol.* 49 (20): 12414–12421. https://doi.org/10.1021/acs.est.5b03111.

Sun, B., D. Li, W. Linghu, and X. Guan. 2018. "Degradation of ciprofloxacin by manganese(III) intermediate: Insight into the potential application of permanganate/bisulfite process." *Chem. Eng. J.* 339 (May): 144–152.

Sun, B., D. Rao, H. Dong, and X. Guan. 2016b. "Comparing the suitability of sodium hyposulfite, hydroxylamine hydrochloride and sodium sulfite as the quenching agents for permanganate oxidation." *RSC Adv.* 6 (16): 13335–13342. https://doi.org/10.1039/C6RA01209D.

Sun, B., D. Rao, Y. Sun, and X. Guan. 2016c. "Auto-accelerating and auto-inhibiting phenomena in the oxidation process of organic contaminants by permanganate and manganese dioxide under acidic conditions: Effects of manganese intermediates/products." *RSC Adv.* 6 (67): 62858–62865. https://doi.org/10.1039/C6RA10196H.

Sun, B., J. Zhang, J. Du, J. Qiao, and X. Guan. 2013. "Reinvestigation of the role of humic acid in the oxidation of phenols by permanganate." *Environ. Sci. Technol.* 47 (24): 14332–14340. https://doi.org/10.1021/es404138s.

Sun, J. H., G. L. Wang, Y. Chai, G. Zhang, J. Li, and J. Feng. 2009. "Distribution of polycyclic aromatic hydrocarbons (PAHs) in Henan Reach of the Yellow River, Middle China." *Ecotoxicol. Environ. Saf.* 72 (5): 1614–1624. https://doi.org/10.1016/j.ecoenv.2008.05.010.

TCEQ. 2017. "Surface water quality web reporting tool." Accessed November 7, 2017. https://www80.tceq.texas.gov/SwqmisPublic/index.htm.

Thabaj, K. A., S. D. Kulkarni, S. A. Chimatadar, and S. T. Nandibewoor. 2007. "Oxidative transformation of ciprofloxacin by alkaline permanganate: A kinetic and mechanistic study." *Polyhedron* 26 (17): 4877–4885. https://doi.org/10.1016/j.poly.2007.06.030.

USEPA. 2009. "US EPA national primary drinking water regulations (NPDWRs)." Accessed October 27, 2017. https://www.epa.gov/sdwa/drinking-water-regulations-and-contaminants#Secondary.

Von Gunten, U. 2003. "Ozonation of drinking water. Part II: Disinfection and by-product formation in presence of bromide, iodide or chlorine." *Water Res.* 37 (7): 1469–1487. https://doi.org/10.1016/S0043-1354(02)00458-X.

Waldemer, R. H., and P. G. Tratnyek. 2006. "Kinetics of contaminant degradation by permanganate." *Environ. Sci. Technol.* 40 (3): 1055–1061. https://doi.org/10.1021/es051330s.

Wang, P., Y. L. He, and C. H. Huang. 2011. "Reactions of tetracycline antibiotics with chlorine dioxide and free chlorine." *Water Res.* 45 (4): 1838–1846. https://doi.org/10.1016/j.watres.2010.11.039.

Xiao, X., S. P. Sun, M. B. McBride, and A. T. Lemley. 2013. "Degradation of ciprofloxacin by cryptomelane-type Mn(III/IV) oxides." *Environ. Sci. Pollut. Res.* 20 (1): 10–21. https://doi.org/10.1007/s11356-012-1026-6.

Yurdakul, S., I. Çelik, M. Çelen, F. Öztürk, and B. Cetin. 2019. "Levels, temporal/spatial variations and sources of PAHs and PCBs in soil of a highly industrialized area." *Atmos. Pollut. Res.* 10 (4): 1227–1238. https://doi.org/10.1016/j.apr.2019.02.006.

Zazo, J. A., J. A. Casas, A. F. Mohedano, M. A. Gilarranz, and J. J. Rodríguez. 2005. "Chemical pathway and kinetics of phenol oxidation by Fenton's reagent." *Environ. Sci. Technol.* 39 (23): 9295–9302. https://doi.org/10.1021/es050452h.

Zhang, J., B. Sun, and X. Guan. 2013. "Oxidative removal of bisphenol A by permanganate: Kinetics, pathways and influences of co-existing chemicals." *J. Sep. Purif. Technol.* 107: 48–53. https://doi.org/10.1016/j.seppur.2013.01.023.

Zimmermann, S. G., M. Wittenwiler, J. Hollender, M. Krauss, C. Ort, H. Siegrist, and U. von Gunten. 2011. "Kinetic assessment and modeling of an ozonation step for full-scale municipal wastewater treatment: Micropollutant oxidation, by-product formation and disinfection." *Water Res.* 45 (2): 605–617. https://doi.org/10.1016/j.watres.2010.07.080.

Zoppini, A., N. Ademollo, M. Bensi, D. Berto, L. Bongiorni, A. Campanelli, B. Casentini, L. Patrolecco, and S. Amalfitano. 2019. "Impact of a river flood on marine water quality and planktonic microbial communities." *Estuarine Coastal Shelf Sci.* 224 (Apr): 62–72. https://doi.org/10.1016/j.ecss.2019.04.038.